

# Activation time imaging of ventricular excitation: a qualitative spatio-temporal feature detector

Liliana Ironi and Stefania Tentoni

IMATI - CNR

via Ferrata 1, 27100 Pavia, Italy

{ironi,tentoni}@imati.cnr.it

## Abstract

The intrinsic diagnostic limitations of traditional ECG's have motivated the development of novel methods for electrocardiac imaging. In particular, body surface potential maps are becoming available, as well as epicardial maps obtained noninvasively from body surface data through mathematical model-based reconstruction methods. Such maps can capture a number of electrical conduction pathologies that can be missed by ECG's analysis, but their introduction into the clinical practice is still far away as their interpretation requires skills that are possessed by very few experts. This paper describes a research effort towards the realization of an automated electrocardiac map interpretation tool. More precisely, its focus is on activation isochrone maps. Starting from original 3D epicardial data gathered over time, we exploit numerical and qualitative information to build the surface maps, and to extract the wavefront propagation and velocity patterns, as well as other salient features that characterize the heart electrical activity. To this end, a set of spatial objects at different abstraction levels is built along with a neat hierarchical network of spatial relations and qualitative functional similarities between them. Spatial Aggregation results to be a natural conceptual framework to define, extract, and make features available for reasoning tasks.

*Keywords:* imaging, qualitative reasoning, spatial reasoning, electrocardiology.

## 1 Introduction

During the last decade, noninvasive functional imaging techniques, such as computerized tomography and magnetic resonance, have increasingly replaced pure anatomical imaging for medical diagnosis as they are capable to provide both very detailed anatomical images and spatio-temporal measures of physiological parameters that characterize the activity of different organ areas. In Electrocardiology, unfortunately, similar directly applicable techniques are not yet available. Nevertheless, the heart electrical function may be noninvasively

evaluated by reconstructing spatio-temporal information of the epicardial activity from body surface mapping.

The research effort currently devoted to the development of novel methods for electrocardiographic imaging [Ramanathan *et al.*, 2004] is strongly motivated by the intrinsic diagnostic limitations of traditional electrocardiograms (ECG's), for which, however, an interpretative rationale is well-established. Infact, ECG's provide only a low resolution projection on the chest surface of the heart electrical activity: on the one hand, due to the distance of the electrodes from the cardiac bioelectric sources, the informative content of the electrical signals recorded on the chest is necessarily weak. On the other hand, when probing is limited to a small number of sites on the chest, as in clinical ECG's protocols, a few electrical conduction pathologies (arrhythmias, infarcts, Wolf-Parkinson-White syndrome just to cite some) may remain undetected.

A higher resolution projection of the cardiac electrical activity is obtained by body surface mapping (BSM): electrical potential is simultaneously recorded from a few hundreds of sites on the entire chest surface over a complete heart beat [Taccardi *et al.*, 1998]. But, the most of information useful to localize anomalous conduction sites is got when mappings of the significant physical variable values are given, and visualized, as close as possible to the heart where such phenomena originate, and where any necessary surgical intervention has to be extremely focussed.

Thanks to the latest advances in scientific computing, given as inputs (i) body surface potentials and (ii) the geometric relationship between the chest and the heart, epicardial electrical data may be noninvasively reconstructed by using mathematical models and numerical inverse procedures [Colli Franzone *et al.*, 1985; Oster *et al.*, 1997]. Moreover, mathematical models are crucial to highlight, through numerical simulation, the links between the observable patterns (effects) and the underlying bioelectric phenomena (causes). Although still progressively being improved, the interpretative rationale for electrocardiac maps defined by expert electrocardiophysicologists with the helpful support of applied mathematicians is significant enough to be actually used. However, its introduction into the clinical practice is not yet at hand because the ability to both extract salient visual features from electrocardiographic maps and relate them to the underlying complex physiological phenomena still belongs to very few ex-

perts [Taccardi *et al.*, 1998]. Thus, the need to bridge the gap between the established research outcomes and clinical practice.

This paper describes a piece of work that fits into a long-term research project aimed at delivering an automated electrocardiac map interpretation tool to be used in a clinical context. To this end, Qualitative Reasoning (QR) methodologies, and the Spatial Aggregation (SA) approach can play a crucial role in the identification of spatio-temporal patterns and salient features in the map. Let us remind that the application of QR methods is not new in Electrocardiology as demonstrated by a number of automated interpretation tools of traditional ECG's [Bratko *et al.*, 1989; Weng *et al.*, 2001; Kundu *et al.*, 1998; Watrous, 1995].

SA is a computational framework specifically designed for reasoning about spatially distributed data [Yip and Zhao, 1996; Bailey-Kellogg *et al.*, 1996; Huang and Zhao, 2000], and provides a suitable ground to capture spatio-temporal adjacencies at multiple scales. Its hierarchical strategy in aggregating spatial objects to abstract a field at different levels emulates the way experts usually perform imagistic reasoning about fields, that is (1) searching for regularities, and (2) abstracting structural information about the underlying physical processes. In outline, SA transforms a numeric input field into a multi-layered symbolic description of the structure and behavior of the physical variables associated with it. This results from successive transformations of lower-level objects into more and more abstract ones by exploiting distinctive qualitative equivalence properties shared by neighbor objects. The main advantage offered by a SA-like method over conventional visualization ones lies in its capability of preserving and representing spatial relations between geometrical objects at different abstraction levels. This facilitates the automated extraction of features and general rules necessary to infer the causal relationships between pathophysiological patterns and wavefront structure and propagation.

This paper is focussed on activation time maps at epicardial level, as they are a synthetic representation of the spatio-temporal aspects of the propagation of the electrical excitation. It describes how the most significant features that characterize such phenomena and reveal either their normality or abnormality, such as wavefront breakthrough and extinction regions, minimum and maximum propagation velocity patterns, are defined within the SA conceptual framework, and extracted from the epicardial electrical data. Let us emphasize that SA-like procedures make information on both the internal structure of objects and neighborhood relations between them available in a structured and hierarchical way. As a consequence, the relevant information for performing reasoning tasks can be promptly located and used.

## 2 Describing ventricular excitation through features abstracted from the activation map

Experimental and model-based studies recently carried out show that the spread of the excitation within the heart is not uniform: both anisotropic conductivity properties and the fiber structure of the tissue affect the wavefront propagation. To investigate this spatio-temporal process electrocardiolo-

gists use a well-established parameter that is also important for the diagnosis of cardiac rhythm, namely the activation time.

*Definition 1.* Let  $\mathbf{x}$  be a point of the myocardium  $\Omega \subset R^3$ , the heart's muscular wall. The *activation time*  $\tau(\mathbf{x})$  is the instant at which the excitation front reaches  $\mathbf{x}$ , causing it to depolarize.

*Definition 2.* An *activation map* is a contour map of the activation time built on a reference surface, where each contour line aggregates all and none but the points that depolarize at the same instant.

Since wavefront propagation is a 3D process, which is quite difficult to be visualized within the volume  $\Omega$ , activation maps are built on reference surfaces, usually the external/internal boundaries of  $\Omega$  (epicardial/endocardial surfaces, respectively), but also transverse and longitudinal intramural sections. The activation time can be either experimentally measured by advanced optical techniques, or computed from the epicardial potential data when these are available over a whole beat. Activation maps contain a lot of information about the wavefront structure and propagation: subsequent isochrones represent the wavefront kinematics as a sequence of snapshots.

The isochrone distributions are complex, with several distinct areas showing different propagation patterns that the expert analysis may reveal: the locations on the considered surface where wavefront breaks through and vanishes, the local fiber direction, the wavefront propagation pathways, and the regions with high, low or null conductivity. Thus, such kinds of maps have a clear and strong diagnostic value: by comparison with a nominal activation map, anomalous conduction patterns and regions with altered conductivity can be easily detected and classified.

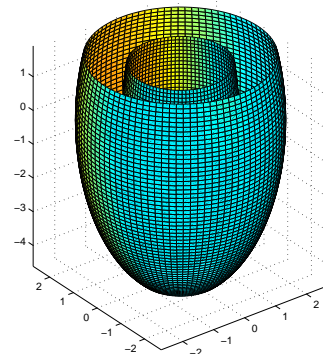


Figure 1: Model ventricle 3D geometry: the mesh is shown on the most external and internal ventricle layers.

Sophisticated mathematical models of the ventricular excitation that take into account both fiber architecture and conduction anisotropy exist [Henriquez, 1993; Henriquez *et al.*, 1996; Roth, 1992; Colli Franzone *et al.*, 1998]. Herein, we consider simulated data obtained by the model proposed by [Colli Franzone *et al.*, 1998]. Figure 1 illustrates a 3D simplified ventricular geometry. Its discretization was carried out by 90 horizontal sections, 61 angular sectors on each section,

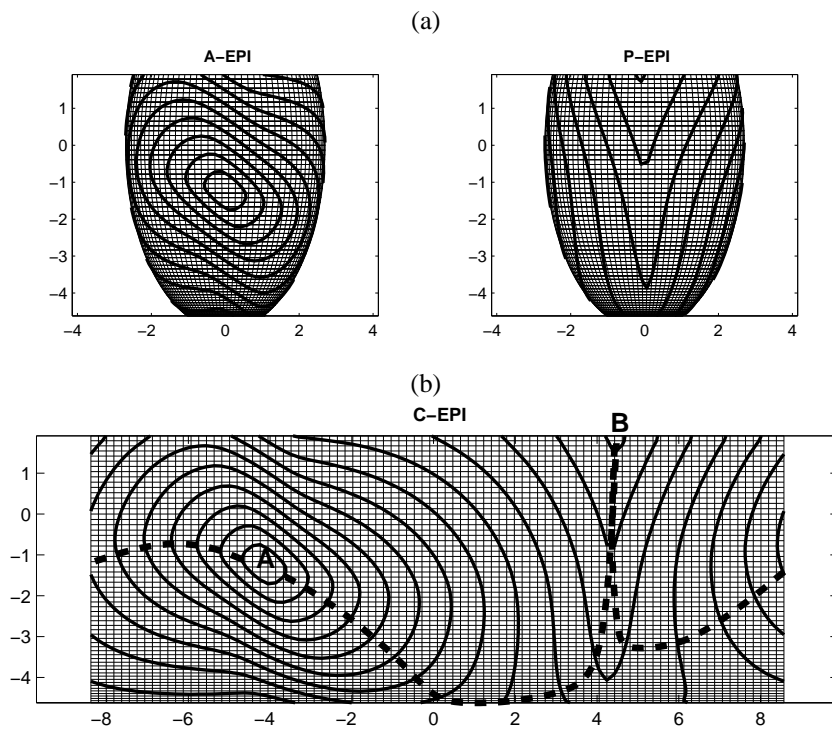


Figure 2: (a) Anterior and posterior orthogonal projections of the activation map (solid thick lines) drawn on the external boundary of the 3D mesh (thin lines). (b) Cylindrical projection of the same isomap; maximum velocity propagation pathways (thick dashed lines) from wavefront breakthrough (A) to extinction (B) locations are sketched.

and 6 radial subdivisions of each sector. A numerical simulation, based on an anisotropic bidomain model of the ventricle tissue, was carried out on this mesh: the potential  $u(\mathbf{x}, t)$  was computed over a whole beat at each node  $\mathbf{x}_i$ . Hence, the activation time  $\tau(\mathbf{x}_i)$  was obtained as the instant of minimum time derivative of each electrogram  $u(\mathbf{x}_i, t)$ .

## 2.1 The feature extraction problem

Contour lines are the first result from processing the input activation time data. Figure 2 highlights what are the pieces of information that we want to extract from contour maps. Figure 2(a) shows the anterior and posterior orthogonal projections of the activation map on the external ventricle boundary. In order to have a unique global view with minimal spatial distortion, we consider a cylindrical projection of this map (Fig.2(b)). Reasoning on panel (b), the expert would: i) identify point A where the excitation starts from, ii) identify regions where contours are more scattered/dense as regions where propagation is faster/slower, iii) sketch the maximum velocity propagation pathway towards the site B where excitation vanishes. Therefore, the *feature extraction problem* is equivalent to the following one: given the activation time field, build an activation map, and search for those geometric patterns or spatial objects that characterize salient aspects of the wavefront propagation process. More precisely,

- given in INPUT:
  - the discretized geometry data, i.e. the set of the surface mesh nodes  $\Omega_h = \{\mathbf{x}_i\}_{i=1..N}$ ,

- the activation data  $\{\tau_i\}_{i=1..N}$ , where  $\tau_i = \tau(\mathbf{x}_i)$ ,
- a time step  $\Delta\tau$  to uniformly scan the time range  $[0, T]$ ;

- provide as OUTPUT:

- the sequence of wavefront snapshots:  $\mathcal{I}_k = \{\mathbf{x} \mid \tau(\mathbf{x}) = k\Delta\tau\}_k$ ,  $k = 1, \dots, n_\tau$
- the wavefront breakthrough region:  $\mathcal{R}_b = \{\mathbf{x} \mid \tau(\mathbf{x}) = \min \tau\}$
- the wavefront extinction region:  $\mathcal{R}_e = \{\mathbf{x} \mid \tau(\mathbf{x}) = \max \tau\}$
- the propagation velocity patterns.

## 2.2 The Spatial Aggregation framework

The problem above, i.e. the extraction of both wavefront structure and propagation from raw epicardial data, is solved through a sequence of intermediate representations that gradually identify the geometric patterns, the spatial relations between them, and the global dynamical behavior. The adopted ontological framework is that one underlying the Spatial Aggregation approach: geometric patterns, or *spatial objects*, are built up from a given input field by applying an iterative procedure that transforms lower-level abstract objects, called *spatial aggregates*, into ones at a higher abstraction level. Neighborhood relations play a crucial role in extracting the necessary structural and behavioral information for performing a specific task: on the one hand, intra-relations bind a set of contiguous spatial aggregates into a single object; on

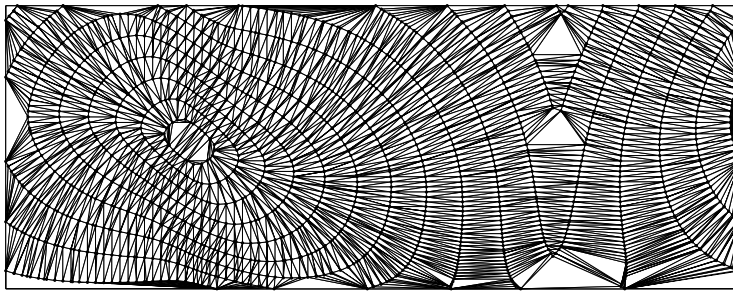


Figure 3: Isopoints (dots) and their ngraph (thin solid lines).

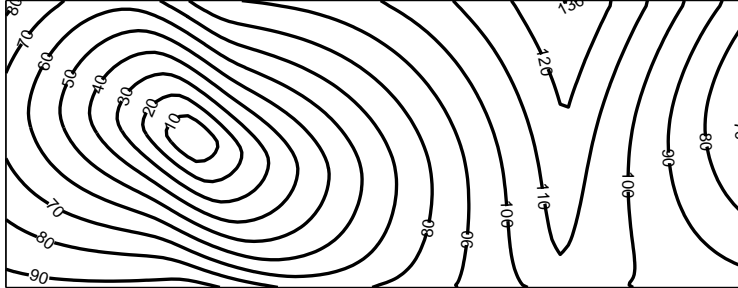


Figure 4: Isochrones abstracted as strong adjacencies between isopoints.

the other hand, inter-relations highlight the connectivity and interactions between the spatial objects aggregated at the previous level. The former kind of relation is called *strong adjacency*, and the latter one *weak adjacency*.

In outline, the overall process iterates three main steps: *aggregate*, *classify*, and *redescribe*. The aggregate procedure makes the spatial contiguity between field objects explicit by encoding it in a *neighborhood graph* (n-graph). Then, the application of a strong adjacency relation on contiguous elements represented by the n-graph defines equivalence classes characterized by a distinctive property. The equivalence classes are finally transformed into new higher-level spatial objects through the *redescribe* operator. The three steps are repeated until the desired structural and behavioral information is obtained.

The hierarchical structure of the whole set of built spatial objects allows us to state a bi-directional mapping between higher and lower-level aggregates, and, then, it facilitates the identification of the piece of information relevant for a specific task.

### 3 Extracting wavefront structure from epicardial data

The isochrone shapes and distributions built on ventricular external and internal surfaces, and on intramural sections, define the wavefront structure. Then, its reconstruction turns into 2D contouring problems.

#### 3.1 From epicardial data to activation isochrone maps

Proper definitions and algorithms to soundly tackle the contouring task for generic geometrical domains within the SA

framework have been given and discussed in [Ironi and Ten-toni, 2003a; 2003b]. In outline, SA contouring is performed in four main steps:

1. Pre-processing of the activation data to generate the set of isopoints  $\mathcal{P}$  for the required levels. The set  $\mathcal{P}$  is built by comparison of the values at the mesh nodes with the required levels, and by linear interpolation of mesh nodal values.
2. Definition of the spatial contiguities between isopoints, i.e. construction of the n-graph  $\mathcal{N}_{\mathcal{P}}$  (Fig. 3). The resulting n-graph must ensure that the spatial contiguity of points in  $\mathcal{N}_{\mathcal{P}}$  also respects their nearness in terms of the associated functional values: a Delaunay triangulation is accordingly adjusted to guarantee a proper representation.
3. Classification of the contiguous isopoints represented in  $\mathcal{N}_{\mathcal{P}}$ .  $\mathcal{P}$  is partitioned into equivalence classes that are built by applying a strong adjacency relation based on topological adjacency properties rather than a metric distance.
4. Construction of the isocurves (Fig. 4). The equivalent classes defined at the previous step are redescribed as polylines, whose vertices are isopoints and whose edges are instances of the strong adjacency relation holding between them. Let us observe that a single wavefront snapshot  $\mathcal{I}_k$  may consist of more connected components  $\mathcal{I}_k^{i_k}$  (see, for example, the isocurve labelled 80 in Fig. 4). Thus,  $\mathcal{I}_k = \cup_{i_k=1, \dots, n_k} \mathcal{I}_k^{i_k}$ , where  $n_k$  is the number of connected components.

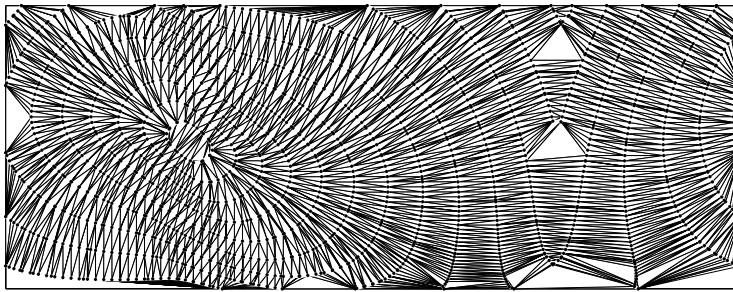


Figure 5: Weak adjacency graph between isopoints.

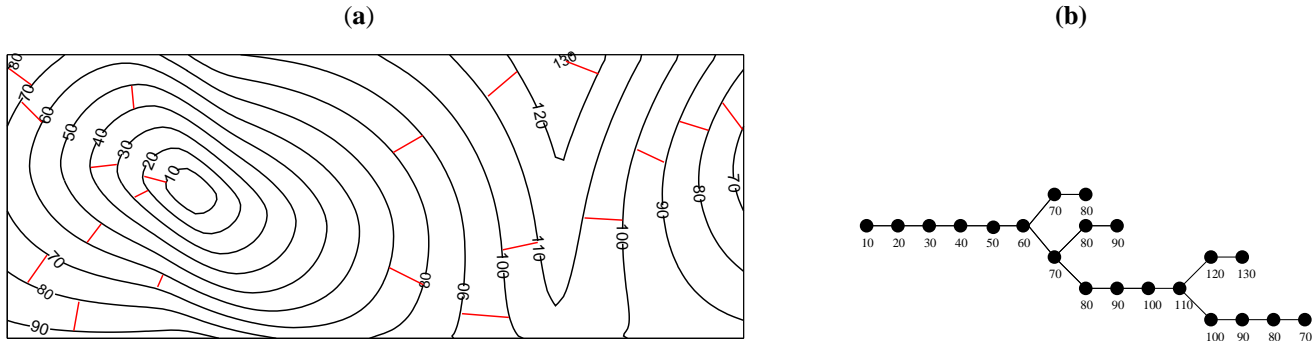


Figure 6: (a) Spatial, and (b) symbolic representation of  $\mathcal{N}_{\mathcal{I}}$ .

### 3.2 Spatial adjacency relations between isochrones

To identify the salient features that characterize wavefront propagation, steps analogous to 2-4 given above are iterated until the relevant pieces of information are made available at the desired high-level as aggregate objects. Then, after isochrones  $\mathcal{I}_k$  have been abstracted by exploiting both contiguity and strong adjacency between isopoints, the next step deals with the construction of a neighborhood graph,  $\mathcal{N}_{\mathcal{I}}$ , that encodes curve contiguity. To this end, a straightforward strategy consists in exploiting weak adjacency relations between isochrone constituent isopoints.

*Definition 3.* Given the set of isopoints  $\mathcal{P}$  and their n-graph  $\mathcal{N}_{\mathcal{P}}$ , we say that  $\mathbf{x}, \mathbf{y} \in \mathcal{P}$  are *weakly adjacent* if they are contiguous within  $\mathcal{N}_{\mathcal{P}}$  but not strongly adjacent (Fig. 5)<sup>1</sup>.

*Definition 4 (n-graph of isochrones).* Two isochrones  $\mathcal{I}'$  and  $\mathcal{I}''$ , with respective time labels  $\tau', \tau''$ , are contiguous if:

- 1)  $|\tau' - \tau''| = \Delta\tau$ , and
- 2) there exists at least one couple of isopoints  $\mathbf{x}, \mathbf{y}$  weakly adjacent, where  $\mathbf{x} \in \mathcal{I}'$  and  $\mathbf{y} \in \mathcal{I}''$ .

Spatial contiguity between isocurves is then represented by  $\mathcal{N}_{\mathcal{I}}$  that encodes any one of these weak connections. Figure 6 depicts a spatial (panel A) and a symbolic (panel B) representation of  $\mathcal{N}_{\mathcal{I}}$ . In the latter representation, graph nodes represent isochrone connected components, and edges state neighborhood relations between them.

<sup>1</sup>Let us highlight that Fig. 5 differs from Fig. 3 as the intra-relations binding isopoints within an isocurve are not considered.

Let us emphasize that the graph  $\mathcal{N}_{\mathcal{I}}$  encodes both a spatial contiguity relation and a temporal order between isochrones.

## 4 Extracting wavefront propagation from isochrone maps

The ordered time sequence of the wavefront snapshots, their velocity properties, as well as the breakthrough and extinction regions are the features that define the wavefront propagation as it is observed on the surface considered.

### 4.1 Breakthrough and extinction regions

The *breakthrough* and *extinction* regions where excitation arises and, respectively, vanishes are easily characterized as the subsets  $\mathcal{R}_b$  and  $\mathcal{R}_e$  of  $\Omega_h$  which are earliest and last activated.

Let us define a *quantity space* of the time variable:

$\mathcal{Q}_\tau = \{\tau_{\min} \tau_{\text{med}} \tau_{\max}\}$ , and a mapping  $q : [0, T] \rightarrow \mathcal{Q}_\tau$  such that  $q : [0, \epsilon] \rightarrow \tau_{\min}$ ,  $q : (\epsilon, T - \epsilon) \rightarrow \tau_{\text{med}}$ ,  $q : [T - \epsilon, T] \rightarrow \tau_{\max}$ <sup>2</sup>.

Let us consider the lowest-level spatial objects defined by the original mesh nodes  $\Omega_h = \{\mathbf{x}_i\}$ . Then, the mesh itself defines the spatial contiguity between points, i.e. the related n-graph, and new spatial objects are abstracted by applying the following strong adjacency relation:

*Definition 5.*  $\mathbf{x}_i, \mathbf{x}_j \in \Omega_h$  are *similarly-activated* if they are contiguous within the mesh AND  $q\tau(\mathbf{x}_i) = q\tau(\mathbf{x}_j)$ .

<sup>2</sup> $\epsilon$  is a suitable numeric tolerance (herein,  $\epsilon = T/100$ )

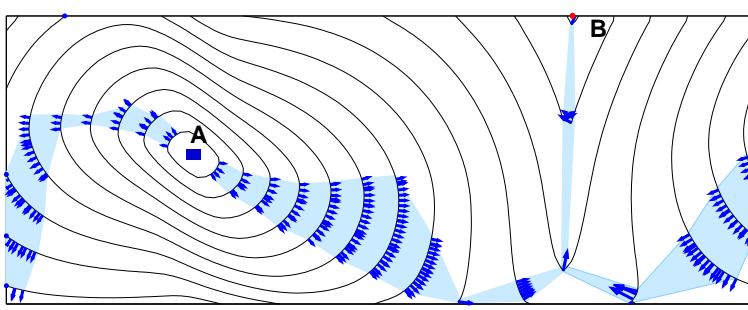


Figure 7: A, B respectively denote breakthrough and extinction regions. Wavefront fragments qualitatively characterized by  $\nu_{max}$  are represented by the set of velocity vectors plotted in their constituent isopoints. Maximum propagation velocity bands are filled in gray.

As a consequence,  $\mathcal{R}_b$ ,  $\mathcal{R}_e$  are the redescribed objects that correspond to the earliest-activated ( $\tau_{min}$ ) and last-activated ( $\tau_{max}$ ) classes. In Figure 7 such regions are labelled A and B, respectively. In this case, B is one single point, located on the top edge of the surface boundary beyond the last contour, while A consists of a whole mesh element whose vertices coincide with the sites where the electrical stimulus was applied.

## 4.2 Propagation velocity bands: a qualitative approach

As the spatio-temporal progression of the isochrones, encoded by  $\mathcal{N}_{\mathcal{I}}$ , is available, we can identify another important feature of the excitation process, that is the wavefront velocity patterns. This is achieved in two main steps by (1) identifying isochrone segments characterized by the same qualitative velocity value, and (2) by classifying them in accordance with their propagation direction. Let us remind that the wavefront motion is a 3D process, therefore the velocity here considered is the wavefront apparent surface velocity along the outward normal to the front. If  $\mathbf{x} \in \mathcal{I}_k$ , its velocity  $\mathbf{v}(\mathbf{x})$  is directed as the outward normal to  $\mathcal{I}_k$ , and has a magnitude  $v(\mathbf{x}) = 1/|\nabla\tau(\mathbf{x})|$ , where  $\nabla\tau(\mathbf{x})$  is the gradient of  $\tau(\mathbf{x})$  and is numerically approximated.

### Algorithm 1. Wavefront fragment extraction.

Let us define a *quantity space*  $\mathcal{Q}_v = \{\nu_{min} \ \nu_{med} \ \nu_{max}\}$  of qualitative values that velocity magnitude may assume.

For each given isochrone  $I$ :

1. Denote by  $v(I)$  the velocity magnitude range, that is:
 
$$v(I) = [V_{min}^I, V_{max}^I] \text{ where } V_{min}^I = \min_{\mathbf{x} \in I} v(\mathbf{x}),$$

$$V_{max}^I = \max_{\mathbf{x} \in I} v(\mathbf{x}).$$
2. Define a mapping  $\mu^I : v(I) \rightarrow \mathcal{Q}_v$  such that
 
$$\mu^I : [V_{min}^I, V_{min}^I + \delta] \rightarrow \nu_{min},$$

$$\mu^I : (V_{min}^I + \delta, V_{max}^I - \delta) \rightarrow \nu_{med},$$

$$\mu^I : [V_{max}^I - \delta, V_{max}^I] \rightarrow \nu_{max}^3.$$

<sup>3</sup> $\delta$  is a suitable numerical tolerance (herein,  $\delta = 0.15 * (V_{max}^I - V_{min}^I)$ )

3. Consider the isochrone constituent points, whose spatial contiguity is encoded by their strong-adjacency graph  $\mathcal{N}_{\mathcal{P}}|_I$ , and define the following relation between them:
 

*Definition.*  $\forall \mathbf{x}, \mathbf{y} \in I$  contiguous within  $\mathcal{N}_{\mathcal{P}}|_I$ , we say that they have the same velocity if  $\mu^I v(\mathbf{x}) = \mu^I v(\mathbf{y})$ .
4. Apply the above relation, build velocity equivalence classes, and call each new object a *front fragment*.
5. Repeat points 1-4 for all isochrones.
6. Denote by  $\mathcal{W}$  the set of all the generated front fragments.

A front fragment is spatially represented by the set of velocity vectors associated with its constituent points. Spatial contiguity of front fragments is inherited from  $\mathcal{N}_{\mathcal{I}}$  and encoded in  $\mathcal{N}_{\mathcal{W}}$  by making each fragment contiguous to all the fragments of contiguous isochrones. Since the constituent points of a front fragment  $w$  have the same qualitative velocity value, we can refer to such value as the front fragment velocity magnitude  $\nu_w \in \mathcal{Q}_v$ .

### Algorithm 2. Propagation velocity pattern extraction.

1. Define the *propagation direction* of a front fragment  $w \in \mathcal{W}$  as the direction of the vector  $\mathbf{u}(w) := \sum_{\mathbf{x} \in w} \mathbf{v}(\mathbf{x})$ .
2. Define a *similarly advancing* relation in  $\mathcal{W} \times \mathcal{W}$  to highlight velocity homogeneities:
 

*Definition.*  $\forall w, w' \in \mathcal{W}$  contiguous within  $\mathcal{N}_{\mathcal{W}}$ , we say that they are related if they are advancing in a similar direction and with same qualitative velocity magnitude:

$$\mathbf{u}(w) \cdot \mathbf{u}(w') > 0 \text{ AND } \nu_w = \nu_{w'}.$$
3. Build equivalence classes and abstract them as new objects that we call *velocity bands*.

Figure 7 shows the features extracted from the given activation time data that are relevant for diagnostic purposes: (i) the propagation velocity pattern, i.e. the front fragments qualitatively characterized by  $\nu_{max}$ , and the resulting  $\nu_{max}$ -bands, (ii) the breakthrough and extinction regions (A and B, respectively).

## 5 Conclusions

This piece of work represents the first step towards the realization of a tool for the automated interpretation of electro-

cardiac maps. Herein, we focus on the extraction, from activation time data given in surface mesh nodes, of spatial objects at different abstraction levels that correspond to salient features of wavefront structure and propagation, namely activation map, breakthrough and extinction regions, front fragments, and propagation velocity bands. Let us remark that the proposed algorithms are not domain dependent but applicable to the more general context of the analysis and interpretation of numerical fields associated with propagation phenomena, e.g. reaction-diffusion systems.

The work is done within the SA conceptual framework, and exploits both numerical and qualitative information to define a neat hierarchical network of spatial relations and functional similarities between objects. Such a network provides a robust and efficient way to qualitatively characterize spatio-temporal phenomena. In our specific case, it allows us to identify the locations where the wavefront breaks through or vanishes, its propagation patterns, and the regions where electrical conductivity properties are qualitatively different. Such pieces of information are essential in a clinical context to diagnose ventricular arrhythmias as they can localize possible ectopic sites and highlight abnormal propagation of the excitation wavefront, such as slow conduction, conduction block, and reentry. With the aim of building a diagnostic tool, more work needs also to be done to identify such phenomena, and to extract additional temporal information from sequences of isopotential maps built from epicardial potential data. Further work will be devoted to design and implement methods for the automated interpretation of activation maps. This requires to define a vocabulary of features, as well as methods for their comparison with the features extracted from different raw epicardial data sets, either simulated or measured. To this end, a necessary step will deal with the detection and filtering of faulty and noisy electrical signals.

## References

- [Bailey-Kellogg *et al.*, 1996] C. Bailey-Kellogg, F. Zhao, and K. Yip. Spatial aggregation: Language and applications. In *Proc. AAAI-96*, pages 517–522, Los Altos, 1996. Morgan Kaufmann.
- [Bratko *et al.*, 1989] I. Bratko, I. Mozetic, and N. Lavrac. *Kardio: A Study in Deep and Qualitative Knowledge for Expert Systems*. MIT Press, Cambridge, MA, 1989.
- [Colli Franzone *et al.*, 1985] P. Colli Franzone, L. Guerri, S. Tentoni, C. Viganotti, S. Baruffi, S. Spaggiari, and B. Taccardi. A mathematical procedure for solving the inverse potential problem of electrocardiography. Analysis of the time-space accuracy from in vitro experimental data. *Math.Biosci.*, 77:353–396, 1985.
- [Colli Franzone *et al.*, 1998] P. Colli Franzone, L. Guerri, and M. Pennacchio. Spreading of excitation in 3-D models of the anisotropic cardiac tissue. II. Effect of geometry and fiber architecture of the ventricular wall. *Mathematical Biosciences*, 147:131–171, 1998.
- [Henriquez *et al.*, 1996] C.S. Henriquez, A.L. Muzikant, and C.K. Smoak. Anisotropy, fiber curvature, and bath loading effects on activation in thin and thick cardiac tissue preparations: Simulations in a three-dimensional bidomain model. *J. Cardiovasc. Electrophysiol.*, 7(5):424–444, 1996.
- [Henriquez, 1993] C.S. Henriquez. Simulating the electrical behavior of cardiac tissue using the bidomain model. *Crit. Rev. Biomed. Engr.*, 21(1):1–77, 1993.
- [Huang and Zhao, 2000] X. Huang and F. Zhao. Relation-based aggregation: finding objects in large spatial datasets. *Intelligent Data Analysis*, 4:129–147, 2000.
- [Ironi and Tentoni, 2003a] L. Ironi and S. Tentoni. On the problem of adjacency relations in the spatial aggregation approach. In P. Salles and B. Bredeweg, editors, *Seventeen International Workshop on Qualitative Reasoning (QR2003)*, pages 111–118, 2003.
- [Ironi and Tentoni, 2003b] L. Ironi and S. Tentoni. Towards automated electrocardiac map interpretation: an intelligent contouring tool based on spatial aggregation. In M.R. Berthold, H.-J. Lenz, E. Bradley, R. Kruse, and C. Borgelt, editors, *Advances in Intelligent Data Analysis V*, pages 397–417, Berlin, 2003. Springer.
- [Kundu *et al.*, 1998] M. Kundu, M. Nasipuri, and D.K. Basu. A knowledge based approach to ECG interpretation using fuzzy logic. *IEEE Trans. Systems, Man, and Cybernetics*, 28(2):237–243, 1998.
- [Oster *et al.*, 1997] H.S. Oster, B. Taccardi, R.L. Lux, P.R. Ershler, and Y. Rudy. Noninvasive electrocardiographic imaging: reconstruction of epicardial potentials, electrograms, and isochrones and localization of single and multiple electrocardiac events. *Circulation*, 96:1012–1024, 1997.
- [Ramanathan *et al.*, 2004] C. Ramanathan, R.N. Ghanem, P. Jia, K. Ryu, and Y. Rudy. Noninvasive electrocardiographic imaging for cardiac electrophysiology and arrhythmia. *Nature Medicine*, pages 1–7, 2004.
- [Roth, 1992] B.J. Roth. How the anisotropy of the intracellular and extracellular conductivities influences stimulation of cardiac muscle. *J. Mathematical Biology*, 30:633–646, 1992.
- [Taccardi *et al.*, 1998] B. Taccardi, B.B. Punske, R.L. Lux, R.S. MacLeod, P.R. Ershler, T.J. Dustman, and Y. Vyhmeister. Useful lessons from body surface mapping. *Journal of Cardiovascular Electrophysiology*, 9(7):773–786, 1998.
- [Watrous, 1995] R.L. Watrous. A patient-adaptive neural network ECG patient monitoring algorithm. *Computers in Cardiology*, pages 229–232, 1995.
- [Weng *et al.*, 2001] F. Weng, R. Quiniou, G. Carrault, and M.-O. Cordier. Learning structural knowledge from the ECG. In *ISMDA-2001*, volume 2199, pages 288–294, Berlin, 2001. Springer.
- [Yip and Zhao, 1996] K. Yip and F. Zhao. Spatial aggregation: Theory and applications. *Journal of Artificial Intelligence Research*, 5:1–26, 1996.